Edge-Coupled Coplanar Waveguide Bandpass Filter Design

Thomas M. Weller, *Senior Member, IEEE*

***Abstract*—This paper describes a new technique for the design of edge-coupled coplanar waveguide (CPW) bandpass filters at microwave and millimeter-wave frequencies. The topology consists of coupled-slot pairs that are symmetric about the center of the CPW line. By applying duality and symmetry, a design methodology is developed that follows the well-known coupled-strip approach. In order to provide filter design guidelines, a spectral domain integral equation analysis was used to characterize coupled slots on silicon with a range of geometrical parameters, through which a series of design curves were generated. Experimental results are given for 10-GHz filters printed on high-resistivity silicon, with bandwidths from 5% to 20%. It is shown how the manner of connecting filter sections can influence the frequency response.**

***Index Terms*—Coplanar waveguides, coupled mode analysis, microwave filters, planar transmission lines.**

I. Introduction

SEVERAL topologies useful for the realization of coplanar waveguide bandpass filters have been reported in recent years. As with microstrip, coplanar waveguide (CPW) filters may be comprised of coupled lines [1], [2], stubs [3], and/or lumped elements [4], [5] and are often based on multilayer configurations [6]. The topology of interest in this work, proposed originally by Menzel [7], is one that uses symmetric pairs of asymmetric coupled slots (Fig. 1). This geometry has the advantages of being uniplanar, not requiring air-bridges for ground equalization, and providing for narrow-band filter design. As noted in [7], the symmetry of the structure also inherently suppresses parasitic radiation. The topology has similarities to the ribbon-of-brick-wall approach described in [2].

The contributions of this paper are to provide a design methodology and design curves for bandpass filters using the geometry given in Fig. 1 and to discuss resonator characteristics as they pertain to filter implementation. The characteristic impedance parameters of the coupled CPW sections are determined using a spectral domain integral equation (SDIE) solution described in [8]. Through a conversion to the dual geometry, and by requiring equal aspect ratios—$S/(S+2W)$ in Fig. 1—for the CPW lines feeding each side of the resonators, it is shown that the well-known coupled-strip bandpass filter design equations can be used. A series of design curves are presented in Section IV, followed by experimental results for 5–20% bandwidth, 10-GHz filters on high-resistivity silicon. It is pointed out that unlike coupled-strip topologies, there is more than one way to interconnect the coupled-CPW sections, and the manner chosen can affect the shape of the frequency response.

Manuscript received February 29, 2000; revised August 23, 2000. This work was supported by Raytheon.

The author is with the Wireless and Microwave Program, Department of Electrical Engineering, University of South Florida, Tampa, FL 33620 USA.

Publisher Item Identifier S 0018-9480(00)10773-2.

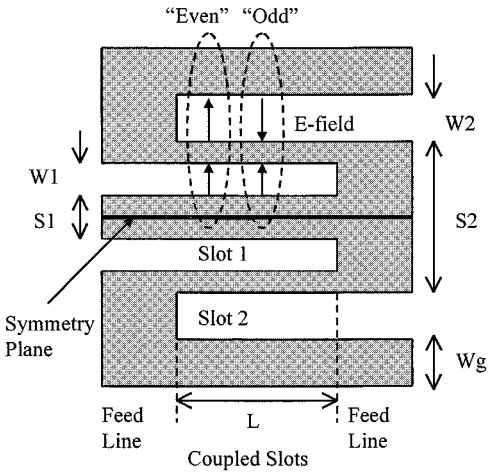

Fig. 1. A single section of an edge-coupled CPW bandpass filter.

II. Coupled-Slot and Dual-Strip Parameters

Assuming an excitation by the odd CPW mode, there are two orthogonal modes that propagate on the coupled-slot geometry in Fig. 1, and magnetic-wall symmetry is maintained along the center of the line. Herein, the two modes on the coupled slots are referred to as "even" and "odd," denoting the relative polarity of the E-field in each slot. In what follows, it is only necessary to treat a single pair of slots on either side of the symmetry plane; this pair is denoted as Slot 1 and Slot 2 in Fig. 1.

The first step in the design procedure is the determination of the even and odd mode characteristics and subsequent conversion to the dual quantities. Using the SDIE method from [8], the even and odd characteristic impedance for each slot ($Z_{e,i}$ and $Z_{o,i}$, $i = 1,2$) are calculated along with the parameters α and κ. The latter are defined as

$$\alpha = \frac{Z_{e,1} \cdot V_{e,2}}{Z_{e,2} \cdot V_{e,1}} \quad \kappa = -\frac{Z_{o,1} \cdot V_{o,2}}{Z_{o,2} \cdot V_{o,1}} \tag{1}$$

where $V_{e,i}$ and $V_{o,i}$ are the even and odd voltages, respectively, on the corresponding slot. The effective dielectric constant (ε_{re}) is assumed to be the same for both modes; from the SDIE simulations, the worst case difference in ε_{re} was found to be 6.7% (for very wide lines) with typical differences below 2.5%.

The dual of the shorted coupled-slot geometry in Fig. 1 is an open circuited coupled-strip geometry. The relationship

between the (even and odd) mode characteristic impedance is given by

$$Z_{e,o(\mathrm{Strip})} = \frac{377^2}{Z_{e,o(\mathrm{Slot})} \cdot 4 \cdot \varepsilon_{re}} \tag{2}$$

where ε_{re} is the effective dielectric constant. In order to convert α and κ to their dual quantities, the following expressions are used [8]:

$$\alpha_{\mathrm{Strip}} = \alpha_{\mathrm{Slot}} \cdot \left(\frac{Z_{e,2,\mathrm{Slot}}}{Z_{e,1,\mathrm{Slot}}} \right) \tag{3}$$

$$\kappa_{\mathrm{Strip}} = \kappa_{\mathrm{Slot}} \cdot \left(\frac{Z_{o,2,\mathrm{Slot}}}{Z_{o,1,\mathrm{Slot}}} \right). \tag{4}$$

III. Filter Design Method

By considering the dual of the coupled *Slot 1–Slot 2* pair, the standard coupled-strip filter design equations [9] can be applied, as long as the geometry is properly constrained. The necessary constraint is to configure the geometry in Fig. 1 such that the image impedance at both ports is identical. This equality of image impedance does not hold in general since the slots in each pair (e.g., *Slot 1* and *2*) are of unequal width and have different offsets from the plane of symmetry. However, it can be shown that by maintaining equal aspect ratios at each port, i.e.,

$$\frac{S_1}{S_1 + 2 \cdot W_1} = \frac{S_2}{S_2 + 2 \cdot W_2} \tag{5}$$

the condition of equal image impedance is indeed met. This relation follows from the fact that (5) forces the characteristic impedance at each port to be the same (assuming ideal quasi-static CPW line behavior [10]) such that the network is electrically symmetric.

As long as (5) is satisfied, the image impedance Z_i and propagation constant β for a (dual) coupled-strip section of electrical length θ are found to be

$$Z_i = \frac{Z_{e,i} - Z_{o,1}}{\alpha + \kappa} \tag{6}$$

$$\cos\beta = (\cos\theta) \cdot \left(\frac{\kappa \cdot Z_{e,1} + \alpha \cdot Z_{o,1}}{Z_{e,1} - Z_{o,1}} \right) \tag{7}$$

assuming two diagonally opposed open-circuited ports in the usual fashion. Equating these parameters to the corresponding ones of an admittance inverter circuit (Fig. 2) at the quarter-wavelength frequency leads to the following:

$$\frac{\kappa \cdot Z_{e,1} + \alpha \cdot Z_{o,1}}{Z_{e,1} - Z_{o,1}} = J \cdot Z_o + \frac{1}{J \cdot Z_o} \tag{8}$$

$$Z_{e,1} - Z_{o,1} = (\alpha + \kappa) \cdot J \cdot Z_o^2. \tag{9}$$

These expressions reduce to those for the symmetric coupled-strip case, for which α and κ are both equal to one.

For completeness, independent tests using SDIE simulation results were performed to measure the validity of (6) and (7). As stated above, these expressions are valid when the two-port coupled-strip section is electrically symmetric, implying that A and D of the ABCD parameters are equal (from which equality of the port 1 and 2 image impedance follows). In terms of the even/odd mode parameters, equality of A and D requires that

$$\frac{\alpha \cdot Z_{e,2} + \kappa \cdot Z_{o,2}}{\kappa \cdot Z_{e,1} + \alpha \cdot Z_{o,1}} = 1. \tag{10}$$

The SDIE simulation results showed this ratio to be consistently between 0.98 and 1.02, when (5) was satisfied.

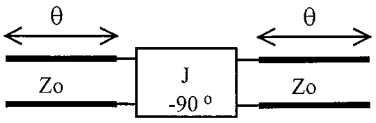

Fig. 2. Equivalent circuit for an individual coupling section in the bandpass filter ($\theta = \pi/2$).

In the work described herein, the effect of substrate and conductor loss has not been included as part of the SDIE formulation. It is possible to account for lossy dielectric materials [11], in which case the resulting complex propagation constant could be applied in a network analysis of the coupled-strip configurations [8], [12]. Without modifying the basic SDIE approach, however, finite thickness and/or finite conductivity lines cannot be analyzed [13].

Based on the analysis presented above, a summary of the design process can be stated.

1) The SDIE method is used to determine even and odd mode characteristics for a given coupled slot geometry, following the constraint given in (5).
2) SDIE results are converted to the dual coupled-strip parameters using (2)–(4).
3) The JZ_o product corresponding to the dual geometry is found using (8).
4) The corresponding value of Z_o for the dual geometry is determined using (9). Since half of the geometry is being treated, this characteristic impedance is half the value of the reference impedance for the actual (dual) coplanar strip feedline.
5) The corresponding Z_o for the original CPW geometry is found using (2) with (two times) the strip Z_o found in the prior step.

In a proper filter design, the necessary geometry of each resonator will provide a particular JZ_o product at a desired reference impedance Z_o. For example, the JZ_o products for the four sections of a third-order bandpass filter are given by [9]

$$J_1 \cdot Z_o = J_4 \cdot Z_o = \sqrt{\frac{\pi \cdot \Delta}{2 \cdot g_1}} \tag{11}$$

$$J_2 \cdot Z_o = J_3 \cdot Z_o = \frac{\pi \cdot \Delta}{2 \cdot \sqrt{g_1 \cdot g_2}} \tag{12}$$

where Δ is the fractional bandwidth and g_i is the low-pass filter prototype element values.

IV. Design Curves

The procedure described above has been repeated on a range of coupled-slot configurations in order to develop design curves. The (SDIE) data pertain to a single frequency of 20 GHz in the center of the band of interest; additional simulations performed

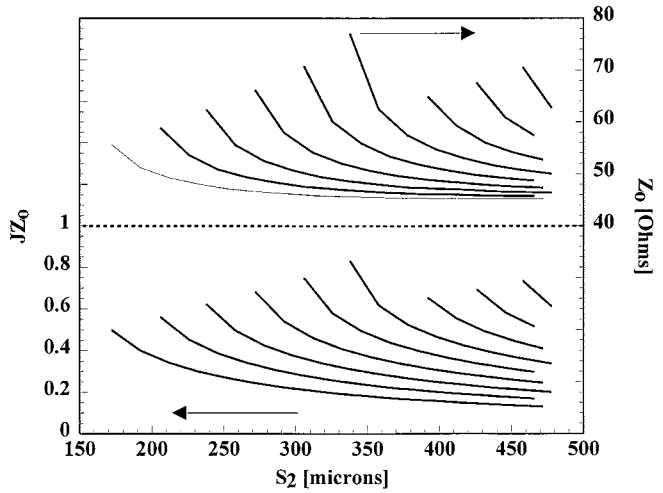

Fig. 3. JZ_o and Z_o values for CPW lines with an aspect ratio of 0.6. Each curve corresponds to a value of S_1 ranging from 80 to 240 μm in steps of 20 μm (moving from left to right).

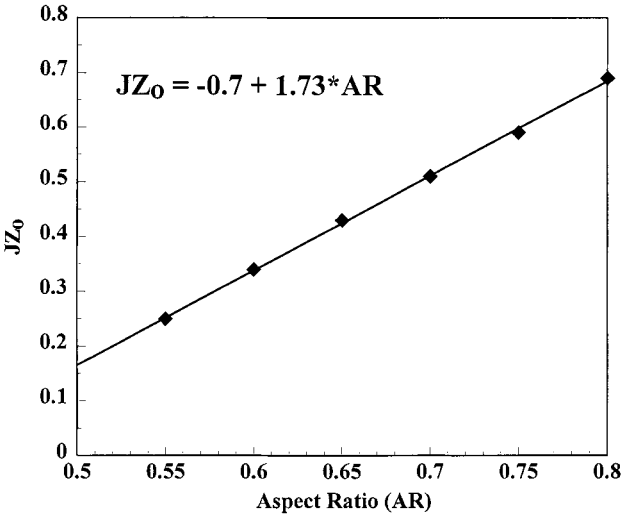

Fig. 4. CPW line aspect ratio versus JZ_o for a 50-Ω reference impedance.

at 10 GHz showed no noticeable differences in the even/odd mode parameters. As it is demonstrated in Section V that dispersion effects are minimal up to at least 40 GHz, quasi-static conditions can be assumed to apply.

A typical set of design curves for the edge-coupled quarter-wavelength CPW resonators is shown in Fig. 3. The data in the figure assume a CPW line aspect ratio of 0.6 at each port, and each curve corresponds to a value of S_1 ranging from 80 to 240 μm in steps of 20 μm (moving from left to right). At any fixed value of S_2, an increase in S_1 reduces the separation between the inner and outer slots; the result is an increase in the coupling, as JZ_o and the corresponding Z_o both increase.

In order to facilitate filter design on silicon using a 50-Ω reference impedance, curve fits of the SDIE results have been generated to determine the necessary line parameters for a given JZ_o product. As shown in Fig. 4, there is a linear relationship between the aspect ratio and JZ_o. Once the aspect ratio has been determined, the necessary value of S_2 for a desired value of S_1 is found from the curves in Fig. 5. Using this design approach

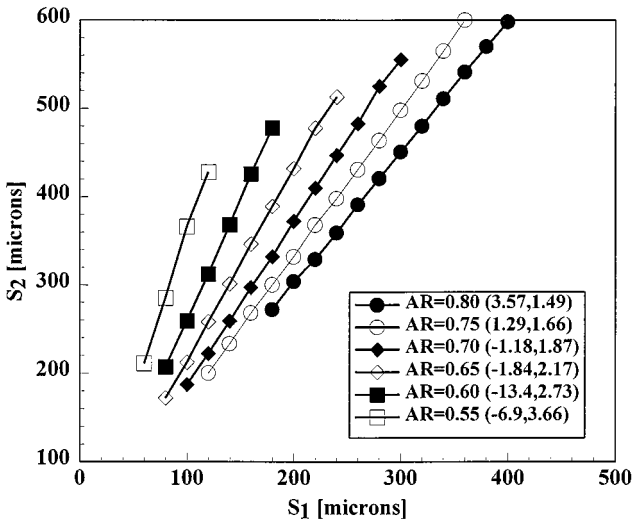

Fig. 5. Relationship between CPW center conductor widths (S_1 and S_2) for different CPW line aspect ratios for a 50-Ω reference impedance. For each aspect ratio (AR) in the legend, the y-intercept and slope of the line are given, i.e., $S_2 = b + m * S_1$.

and assuming that JZ_o values are determined from equations such as (8) and (9), the only free parameter in the geometry of each filter section is S_1.

In reporting design curves such as those in Figs. 3–5, it is common to normalize the parameters so as to provide scalability versus the effective dielectric constant. This approach was not adopted herein in order to preserve the accuracy for the data specifically related to a standard, finite thickness (400 μm) silicon substrate ($\varepsilon_r = 11.7$). As many of the filter sections have lateral dimensions that are nearly twice the thickness of the substrate, the effective dielectric constant can vary by as much as 10% from narrow to wide sections. Use of a thicker silicon substrate would reduce geometry dependence in this regard and also minimize actual differences in the even/odd mode propagation velocities. When using substrates with different dielectric constants, a scaling of Z_o by $(6.5/\varepsilon_{re})^{0.5}$, where ε_{re} is the approximate effective dielectric constant on the substrate of choice, was found to provide reasonable accuracy. Given the lateral width of the designs, particularly when the CPW ground plane dimensions are included, a grounded substrate should not be used in order to avoid parallel plate mode-type resonances.

V. Resonator Characteristics

Resonator characteristics are presented to validate the accuracy of the stated design parameters and also to introduce a point regarding the cascading of individual sections in multi-section filter layouts. A back-to-back configuration of identical $\lambda/4$-sections has been used in order to accommodate measurements/calibration using on-wafer probing. Representative illustrations of the symmetric resonator pairs are given in Figs. 6 and 7. In the former, an "inside-out" configuration is used, denoting the manner in which the slots are coupled when viewed from either port, while in the latter an "outside-in" approach is used.

The results shown in Fig. 8 provide a comparison between measured S-parameters of a CPW resonator pair and the simulated response of a pair of ideal (lossless and nondispersive)

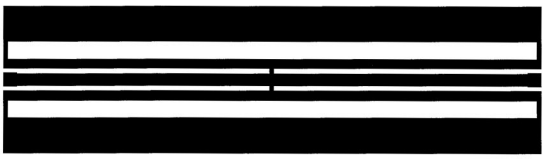

Fig. 6. Symmetric pair of edge-coupled resonators in an "inside-out" configuration.

Fig. 7. Symmetric pair of edge-coupled resonators in an "outside-in" configuration.

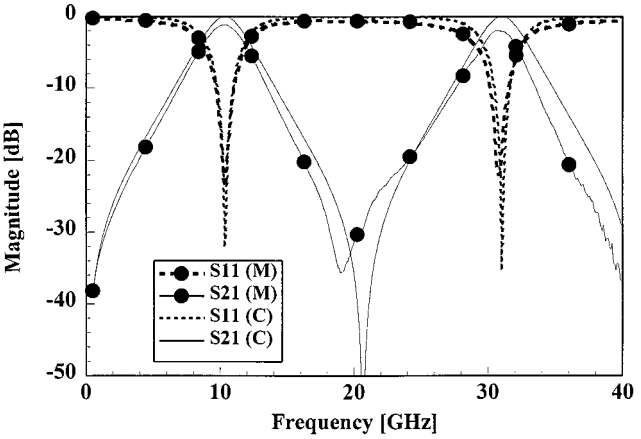

Fig. 8. Comparison between measured characteristics of (inside-out) pair of CPW edge-coupled resonators (M) and symmetric pair of ideal coupled lines (C). The JZ_o product for all resonators is 0.5.

coupled transmission lines. The ideal coupled lines were defined using the even and odd mode characteristic impedance for the corresponding JZ_o (in this case, it is 0.5), and no additional elements were added to emulate discontinuity effects. At 40 GHz, where the maximum CPW resonator width (S_2+2*W_2) for this design approaches $\lambda_g/6$, the comparison to the ideal response is still very good. The fact that quasi-TEM behavior is maintained indicates that the range of values in the design curves presented earlier should be usable into the millimeter-wave frequency band.

Comparisons of the frequency response of the inside-out and outside-in configurations are given in Figs. 9 and 10. Each figure contains curves corresponding to inside-out configurations with JZ_o products of 0.7, 0.5, and 0.2 and outside-in configurations with JZ_o products of 0.4 and 0.2. The measured S_{11} for all resonator pairs appears symmetric about the center frequency of 10 GHz. In contrast, there are significant differences in S_{21} outside the passband—by comparing the two $JZ_o = 0.2$ designs, it is seen that the outside-in arrangement results in a markedly more asymmetric response. These differences may be due in part to physical discontinuities in the slot pattern that are more pronounced in the outside-in configuration (e.g., see Figs. 6 and 7). Since the responses of the $JZ_o = 0.2$ designs differ even around 1 GHz, however, it is likely that discontinuity effects are

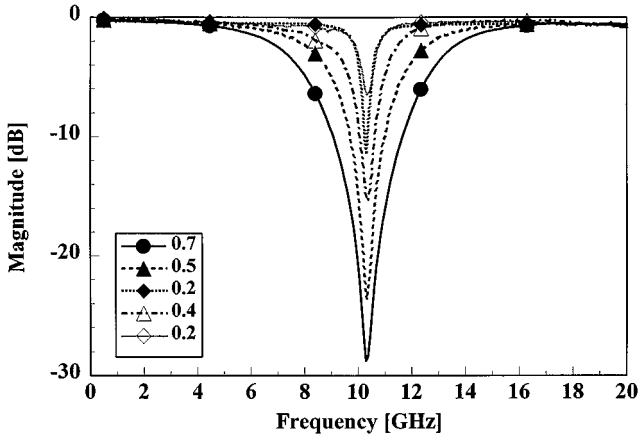

Fig. 9. Measured S_{11} of pairs of CPW edge-coupled resonators for different JZ_o products. For JZ_o equal to 0.7, 0.5, and 0.2, the inside-out configuration is used; the outside-in configuration is used for the other two circuits.

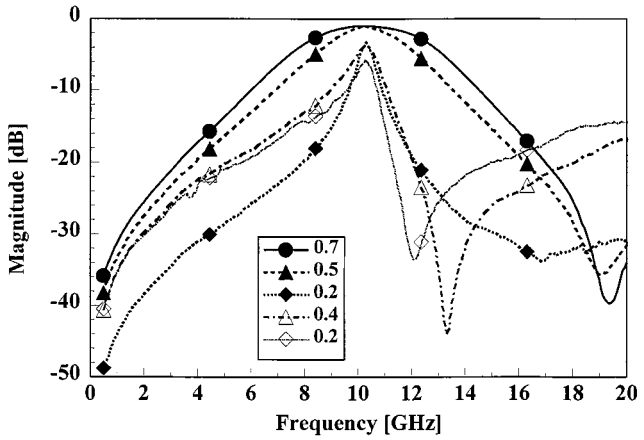

Fig. 10. Measured S_{21} of pairs of CPW edge-coupled resonators for different JZ_o products. For JZ_o equal to 0.7, 0.5, and 0.2, the inside-out configuration is used; the outside-in configuration is used for the other two circuits.

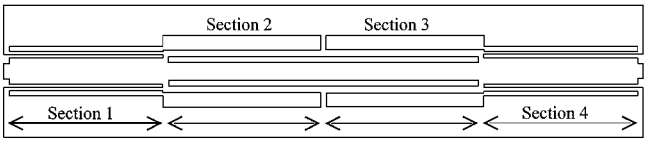

Fig. 11. Layout of a third-order edge-coupled CPW filter. The first and fourth sections use the inside-out configuration, and the second and third use the outside-in configuration.

not the major contributor. As discussed below, the asymmetry characteristic deserves consideration in the design of multisection filters.

VI. Filter Demonstration

Filter designs with bandwidths ranging from 5% to 20% were tested in order to validate the design curves over their full range of parameter values and to examine insertion loss characteristics. A representative layout of a third-order filter is provided in Fig. 11. Each filter was based on a 0.1 dB-ripple Chebyshev response with a center frequency of 10 GHz; the design parameters are given in Table I. The length of each section is slightly less than 90° at 10 GHz (2800 versus 2940 μm, using

TABLE I
CHARACTERISTICS OF FOUR 10-GHz CPW EDGE-COUPLED BANDPASS FILTERS. THE SUBSTRATE IS 400-μm-THICK HIGH—RESISTIVITY ($> 1500\,\Omega$-cm) SILICON ($\varepsilon_r = 11.7$) AND THE METAL IS Cr/Ag/Cr/Au WITH A TOTAL THICKNESS OF 1 μm. IL IS THE MINIMUM MEASURED IN-BAND INSERTION LOSS. ALL DIMENSIONS ARE GIVEN IN MICROMETERS

	Order, BW	Ripple (dB)	IL (dB)	Section	JZo	Length	S1	W1	S2	W2	Wg
Filter 1	3, 20%	0.1	2.2	1 & 4	0.7	2800	240	30	360	45	375
				2 & 3	0.4	2800	160	53	390	130	275
Filter 2	3, 10%	0.1	3.4	1 & 4	0.5	2800	180	38	340	73	357
				2 & 3	0.2	2800	80	40	360	180	240
Filter 3	3, 5%	0.1	5.4	1 & 4	0.35	2800	120	40	300	100	350
				2 & 3	0.1	2800	40	25	300	183	267
Filter 4	5, 20%	0.1	4.8	1 & 6	0.5	2800	180	38	340	73	357
				2 & 5	0.25	2800	100	40	340	140	290
				3 & 4	0.20	2800	80	40	360	180	240

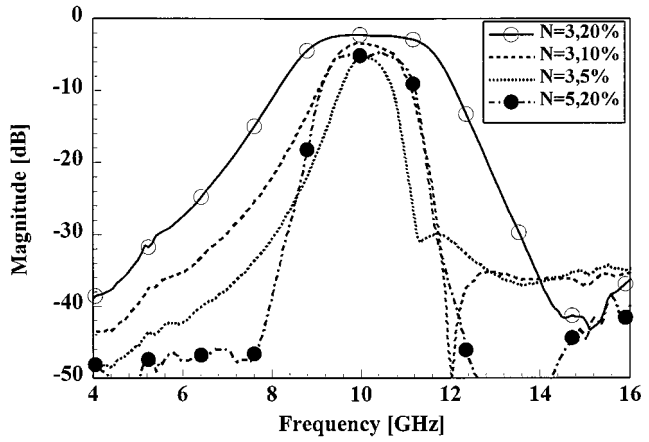

Fig. 12. Measured S_{21} for the four CPW edge-coupled filters listed in Table I.

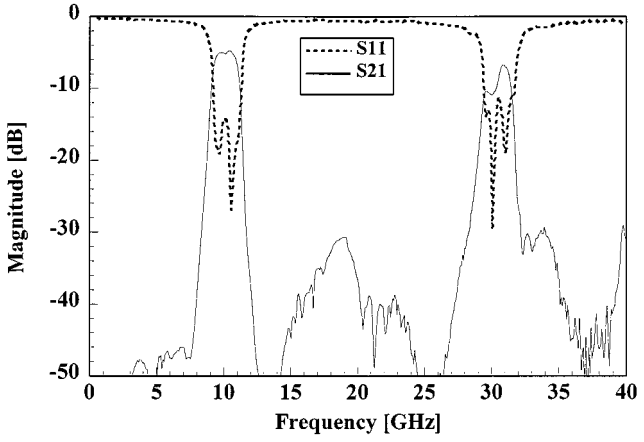

Fig. 13. Measured S-parameters for the fifth-order filter listed in Table I.

$\varepsilon_{re} = 6.5$) to compensate for the short transition between sections. Otherwise, no compensation, such as for end-effect reactance, was included. The filters were fabricated on a bare 400-μm-thick high-resistivity silicon wafer ($\rho > 1500\,\Omega$-cm) using a Cr/Ag/Cr/Au metallization with a total thickness of 1 μm. In order to approximate the finite substrate condition assumed in the SDIE simulations, the circuits were supported on mounts that provided a 1-mm air gap between the substrate and the wafer probe-station chuck during on-wafer testing.

A comparison of measured S_{21} data of the four filters is given in Fig. 12. The minimum insertion loss ranges from 2.2 to 5.4 dB as the bandwidth decreases from 20% to 5%. Identical designs scaled in length for operation at 20 GHz showed 0.2–0.5 dB improvement in the loss, owing to a decrease in the metal skin depth (1 μm translates into 1.5 skin depths at 10 GHz, using the metal system described above). The return loss for all designs was greater than 15 dB in the passband. Broadband characteristics for the fifth-order filter are shown in Fig. 13.

Greater symmetry in the filter frequency response can be achieved by modifying the coupling-section interconnects from the approach shown in Fig. 11. The outside-in configuration used for the interior sections leads to a slight tilting of the passband S_{21} and an enhanced notch on the right side of the skirt; this effect is evident in the response of the 10% and 5% bandwidth filters shown in Fig. 12. While the increased notch may be desirable in applications such as image frequency rejection, it is also possible to remove the asymmetry by reconfiguring the interior sections to be in the inside-out arrangement. This change is affected in a third-order (four-section) filter by connecting the outer slot of section 1 (4) to the inner slot of section 2 (3), rather than connecting the outer slots together. The approach was verified using full-wave simulations, from which it was also found that the rejection at $2f_o$ improved.

VII. SUMMARY

A new technique for the design of narrow-band edge-coupled CPW bandpass filters has been described. Given the even/odd characteristics of the coupled-slot sections, and following a single constraint to maintain equality in the image impedance at each port, it was shown that the standard coupled-strip design equations are applicable to the dual geometry. The topology has compact lateral dimensions, requires no extrinsic ground plane equalization, e.g., air-bridges, and is relatively free of discontinuity effects. These factors simplify design and fabrication in comparison to alternative topologies comprised of shunt stubs or open-circuited discontinuities. It is believed that the design curves presented in this paper are suitable for filter center frequencies to at least 40 GHz.

ACKNOWLEDGMENT

The author thanks the USF Center for Microelectronics Research for providing access to cleanroom facilities used for filter fabrication.

REFERENCES

[1] F.-L. Lin and R.-B. Wu, "Comparative performance of three different CPW bandpass filters," in *1997 IEEE MTT-S Dig.*, pp. 813–816.

[2] F.-L. Lin, C.-W. Chiu, and R.-B. Wu, "Coplanar waveguide bandpass filter—A ribbon-of-brick-wall design," *IEEE Trans. Microwave Theory Tech.*, vol. 43, July 1995.

[3] K. Hettak *et al.*, "Very compact lowpass and bandpass filters using uniplanar structures," in *Proc. 1993 EUMC*, pp. 238–240.

[4] A. Sheta *et al.*, "A new semi-lumped microwave filter structure," in *1995 IEEE MTT-S Dig.*, pp. 383–386.

[5] T. M. Weller, K. J. Herrick, and L. P. B. Katehi, "Quasistatic design technique for Mm-wave micromachined filters with lumped elements and series stubs," *IEEE Trans. Microwave Theory Tech.*, vol. 45, pp. 931–938, June 1997.

[6] W. Schwab and W. Menzel, "Compact bandpass filters with improved stop-band characteristics using planar multilayer structures," in *1992 IEEE MTT-S Dig.*.

[7] W. Menzel, W. Schwab, and G. Strauss, "Investigation of coupling structures for coplanar bandpass filters," in *1995 IEEE MTT-S Dig.*, pp. 1407–1410.

[8] T. Weller, "Micromachined High Frequency Transmission Lines on Thin Dielectric Membranes," Ph.D. dissertation, University of Michigan, 1995.

[9] G. Matthaei, L. Young, and E. M. T. Jones, *Microwave Filters, Impedance-Matching Networks and Coupling Structures*. Reading, MA: Artech House, 1980.

[10] C. P. Wen, "Coplanar waveguide: A surface strip transmission line suitable for nonreciprocal gyromagnetic device applications," *IEEE Trans. Microwave Theory Tech.*, vol. MTT-17, Dec. 1969.

[11] H. Hasegawa *et al.*, "Properties of micro-striplines on Si-SiO2 system," *IEEE Trans. Microwave Theory Tech.*, vol. MTT-19, pp. 869–881, Nov. 1971.

[12] T. Itoh, *Numerical Techniques for Microwave and Millimeter-Wave Passive Structures*. New York: Wiley, 1989, p. 335.

Thomas M. Weller (S'92–M'95–SM'98) received the B.S., M.S., and Ph.D. degrees in electrical engineering from the University of Michigan, Ann Arbor, in 1988, 1991, and 1995, respectively.

He is currently an Assistant Professor in the Electrical Engineering Department, University of South Florida, Tampa. His research involves micromachining applications for microwave and millimeter-wave circuits, packaging, electromagnetic modeling, and millimeter-wave sensors. He has published more than 70 papers in his field.

Dr. Weller was a corecipient of the 1996 Microwave Prize from the IEEE MTT Society.